Original

Surface Area and Porosity Development on Granular Activated Carbon by Zirconium: Adsorption Isotherm Studies

V. Sivanandan Achari[*], A. S. Rajalakshmi, S. Jayasree, Raichel Mary Lopez

*School of Environmental Studies, Cochin University of Science and Technology,
Kochi-682022, Kerala, India.*

Abstract: In this study, a new series of coconut shell based granular activated carbons (GAC) are prepared by impregnating with zirconium ions as zirconyl chloride and activated under superheated steam. These carbons are designated with activation temperature/ conditions as GAC 383 (activated at 383K), GACO 383 (HNO$_3$ oxidised), GACZR 1273 (ZrOCl$_2$ activated at 1273K) and GACOZR 1273 (HNO$_3$ oxidised, ZrOCl$_2$ activated at 1273K). Surface characteristics of these carbons are evaluated using Boehm titration methods, Fourier-transform infrared spectroscopy (FTIR), X-ray diffraction techniques (XRD), Scanning electron microscopy (SEM) and Transmission electron microscopy (TEM). The pore volume and the respective specific surface area of each carbon are determined by BET, I plot, Langmuir, Freundlich, and Dubinin-Radushkevich isotherms using N$_2$ adsorption data at 77K. Analysis shows that zirconium ion enhances the surface area and porosity of granular activated carbon. The adsorption characteristics of newly prepared GAC are tested by solid-liquid equilibria using phenol as adsorbate. Equilibrium phenol adsorption data fitted to standard isotherm models of Langmuir, Freundlich, and Dubinin-Radushkevich (D-R) equations. Adsorption constants and parameters indicate that zirconium impregnated granular activated carbons are relatively more efficient for the removal of phenol than the native carbon used.

Keywords: Adsorption, Granular activated carbon, Phenol, Pore volume, Surface area

1. INTRODUCTION

Activated carbons are regarded as one of the most important commercial materials, with many unique properties with large specific surface areas, high porosity, and adequate pore size distributions. Also, they mostly have high mechanical strength to be used for separation, purification and catalysis (Hameed, Din, & Ahmad, 2007). Activated carbons are produced from many carbonaceous materials of lignocellulosic in origin; this includes coal, wood, peat and agricultural materials (Rodriguez-Reinoso, Molina-Sabio, & Munecas 1992).

Granular activated carbons (GAC) in various forms are quite widely employed in water and wastewater treatment processes for removing organic compounds including phenol and its derivatives (Tan, Ahmad, & Hameed, 2008). Most carbonaceous materials available in nature can be converted into active carbons, differ by their porosity and specific surface area. Depending upon the nature of raw material used and the condition of the activation process chosen, properties of the final carbon product vary. Also, surface modifications of many carbon materials leads to generate more active sites on their solid surface, can be suitably utilized for effective adsorption

[*] Corresponding author.

E-mail address: vsachari@gmail.com (V. Sivanandan Achari).

http://

removal and separation purposes. Such carbons are used as a substitute for other more expensive ion exchange resins, adsorbents and catalyst support (Liu, Zheng, Wang, Jiang, & Li, 2010; Mohd Din, Hameed, & Ahmad, 2009). Literature on carbon science discuss a multitude of activating agents extensively known employed for the production of activated carbon materials with desired pore structure. The purpose of physical/chemical activation is to create and develop porosity in the carbon material and thereby increase their adsorption efficiency. This enhanced porous surface quality has been exploited for the removal of many organic compounds from solutions particularly using coconut shell based carbons (Shen, Li, & Liu, 2008).

All the known carbon activation procedure belongs into two types, namely, physical activation or chemical activation depending on whether a gaseous or the chemical activating agent is used. Chemical activation is a single step process for the preparation of activated carbon where carbonization of precursor in the presence of chemical agents is done under controlled conditions in a furnace. For this, a solid activating agent like alkali and alkaline earth metal containing substances or some acids are used (e.g. KOH, NaOH, Li_2CO_3, Na_2CO_3, K_2CO_3, Rb_2CO_3, Cs_2CO_3, $ZnCl_2$, and H_3PO_4). Physical activation involves two steps, namely (i) carbonization of the precursor in an inert atmosphere (ii) subsequent activation of the resulting char in the presence of carbon gasification agents such as carbon dioxide, steam, air or a suitable combination of these (Namasivayam & Kadirvelu, 1997). However, the impregnation of metal ion/salts onto char matrix modifies the porous structure of resulting activated carbon. An increase in the adsorption efficiency was given by metal ions impregnated carbon for the removal of mercury, lead, arsenic, chromium, Nickel etc. (Sreedhar, Madhukumar & Anirudhan, 1999). Innovative approach regarding activation of carbon with new catalysts is an area of active research in adsorption science.

Zirconium and its salts are reported to be relatively safe and acceptable inorganic substance, has low biotoxicity and are relatively inexpensive. The most important characteristics of this material is their catalytic potential, high reactivity, large specific surface area, ease of separation, and the presence of a large number of active sites for interaction with different contaminants (Holmes, Fuller, & Gammage, 1972). Adsorption performances of various activated carbons with respect to phenol removal have been reported in many earlier studies

(Achari & Anirudhan, 1995; Stoeckli, López-Ramón, & Moreno-Castilla, 2001). An active carbon granule with remarkable porous structure has many advantages over the native carbon form, with respect to porosity and adsorption capacity. In this study, we report the adsorption efficiency of coconut shell based granular activated carbon (GAC) incorporated with zirconium (as $ZrOCl_2$) that resulted extra porosity during thermal activation. Adsorption efficiency of the new activated carbon has been tested with phenol in aqueous phase as regards to study of solid –liquid equilibria.

Phenol is a common organic pollutant and its maximum concentration level in the industrial effluents for safe discharge into surface water bodies is 1.0 mg/L (EPA, 2002). WHO recommends a permissible phenol concentration of 0.001mg/L in potable waters (WHO, 1963). The main sources of phenol in aquatic environments are the wastewater discharges from industries; mainly coke ovens in steel plants, petroleum refineries, resin, petrochemical, fertilizer, pharmaceutical, chemical and dye industries (Girish & Murty, 2012).

The current study is done with a purpose to correlate the effect of Zr^{4+} ions onto native carbon (GAC 383) to generate extra porosity, how it effect the surface complexes, porosity and pore size distribution of activated carbon. The study also discusses the adsorption behaviour of zirconium impregnated carbon for the removal of phenol from aqueous solution.

2. METHODOLOGY

The activated carbon purchased from Indo German Carbon Limited, Binanipuram, Cochin, Kerala, India [particle size (US mesh) 12 x 40, iodine No. 1100 mg/g, apparent density 0.50 g/cc, moisture 5%, ash 4 %] was used throughout the study as the starting material. It was washed with 0.5M NaOH solution and repeated with 0.5M HCl. Finally, more than 1L bed volume of distilled water is passed through a glass column until a neutral pH was noted. Washed carbon was then dried in a hot air oven at 110^0C; it is designated as GAC 383. A portion of this carbon was then nitric acid treated for surface oxidation.

The oxidation of GAC was done in a reaction mixture consisting of 100 g acid washed activated carbon, 130ml of con.HNO_3 and 540ml of distilled water, it is refluxed for 3 hours. After filtration, the procedure was repeated by adding a fresh solution of HNO_3 and distilled water in the

same ratio as the previous. After oxidation, carbon filtered and thoroughly washed with distilled water and dried in a hot air oven at 110⁰C. This nitric acid oxidised granular activated carbon is designated as GACO 383.

2.1 IMPREGNATION RATIO OF ZIRCONIUM

Different weights of zirconyl chloride (ZrOCl₂.8H₂O) noted as the impregnation ratio (I$_{Zr}$ = weight of salt to carbon weight for every 10g carbon) 0.0065, 0.026, 0.052 and 0.078 were used for surface loading. This was done by mixing the raw carbon and activating agent zirconyl chloride at 85⁰C for 2 hours using magnetic stirrer. After stirring samples were placed in a water bath for about 5-6 hours and finally dried in a hot air oven at 110⁰C.

All these impregnated carbons were activated under steam at 873K for choosing the best impregnation ratio for better efficiency in a temperature programmed furnace designed/maintained in the laboratory. The samples with best impregnation ratio, were further activated under steam at a higher temperature of 1273K. This granular activated carbon impregnated with Zr⁴⁺ is designated as GACZR 1273. Similarly, carbon GACOZR 1273 (carbon oxidized zirconyl chloride impregnated and activated at 1273K) was also prepared.

Granular activated carbons

Four carbon samples used for characterization and adsorption studies are designated as GACZR 1273, GACOZR 1273, GAC 383 and GACO 383, being ZR for zirconium and the last figures are for activation temperatures.

The granular activated carbon (GAC) prepared were assigned by the degree of burn off, which was calculated as follows (Ngah & Fatinathan, 2006).

$$Burn\ off\ (\%) = \frac{W_{initial} - W_{final}}{W_{initial}} X\ 100 \qquad (1)$$

W$_{initial}$ is the initial weight of GAC; W$_{final}$ is the weight of GAC after activation.

2.2 CARBON CHARACTERIZATION AND ANALYTICAL METHODS

Surface characterization of newly prepared carbons was performed using FTIR (Thermo Nicolet, Avatar 370) spectroscopy for analyzing the surface functional groups. Boehm's titration method was used for their quantitative determination. In this method, the number of acidic sites,

namely carboxylic, lactonic, and phenolic groups on the carbon surface were distinguished by neutralization with bases (NaHCO₃, Na₂CO₃, NaOH). Their basic character was determined by neutralization with HCl. XRD analyzer (Bruker AXS D8 Advance) was used to measure powder X-ray diffraction patterns of the new GAC series. Scanning Electron Microscope (JOEL Model JSM - 6390LV) and High-Resolution Transmission Electron Microscopy (JOEL/JEM 2100) were used for the study of surface morphological features of carbon material.

2.3 SOLID-GAS EQUILIBRIA STUDIES

The pore structure characteristic of the new activated carbon series was determined by N₂ adsorption-desorption isotherm at 77K volumetrically using Micromeritics TriStar 3000 V6.07 BET analyzer. Isotherm data were subjected to BET, I point, Langmuir, Dubinin-Radushkevich (D-R), t plot and BJH isotherm methods for the determination of pore volume and specific surface area.

2.4 BATCH EQUILIBRIUM ADSORPTION STUDY

Batch test reactors are used for the adsorption studies. 25 ml aqueous solutions of known concentrations of phenol [25, 50, 75, 100, 150, 200, 250, 35, 500, 750, 1000, 1250, 1500, 2000, 2500 & 3000 mg/L] were prepared and added to 0.025g of GAC in a 100 ml Erlenmeyer flask and placed in a temperature-controlled water bath shaker (model LABLINE). The solution was withdrawn from the shaker at the predetermined time interval, filtered through Whatmann No.1 filter paper prior to analysis. The concentration of the phenol in aqueous solution is determined using uv–visible spectrophotometer (CARY 50 Probe) at wavelength 260 nm. The amount of phenol adsorbed at a time t, represented as q_t (mg/g) and adsorbed at equilibrium condition, q_e (mg/g) was calculated according to the following Eq.(2) and Eq.(3) (Gebresemati, Gabbiye, & Sahu, 2017; Kyzas, Deliyanni, & Matis, 2016; Srivastava, Swamy, Mall, Prasad, & Mishra, 2006).

$$q_t = \frac{V(C_0 - C_t)}{W} \qquad (2)$$

$$q_e = \frac{V(C_0 - C_e)}{W} \qquad (3)$$

Where C_0 and C_e are initial and equilibrium phenol concentrations (mg/L) respectively. C_t is phenol concentration at time t (mg/L). V is the volume of solution *(L)* and W is the mass of carbon. An adsorption isotherm profile describes the interaction between adsorbate and adsorbent and is critical for the design of adsorption process. The Langmuir, Freundlich and Dubinin-Radushkevich (D-R) isotherms models were used to describe the equilibrium adsorption isotherm data.

3. RESULTS AND DISCUSSION

3.1 IMPREGNATION RATIO AND BURN OFF

Burn off value of a carbon impregnated with a metal catalyst is the weight loss occurred during the process of activation. Figure 1 shows that burn off found to increase with the amount of zirconium (as zirconyl chloride) loaded. An incorporation of 0.2 % zirconium results 13.1% burn off. Active carbon formed by low burn off are usually undesirable as they lead to a low surface area carbon product, which in turn may reduce adsorption capacity for the target molecule. In the present study burn off is in the range 13-17 % given in Table 1. Development of microporosity occurs in carbon char without a noticeable increase in the micropore width when the burn off value is in between 10- 25% (Molina-Sabio et al., 2006).

The optimum carbon yield 84.72 % with a burn off of 15.28 % is given by an impregnation of 1.5% zirconium, indicate a stage of progressive carbonization (Figure 1). Further incorporation of Zr^{4+} (2.2%) exhibited marked enhancement in burn off (17.28 %) leads to results a lower carbon yield (82.72 %), It is presumed that the impregnation of 1.5 % attributes to a better carbon yield due to uniform distribution and large dispersion of Zr^{4+} ions throughout the accessible interior of the carbon granules.

Based on this observation, 1.5 % of Zr^{4+} impregnated carbon char are used for activation at temperature 1273K for better yield and burn off to obtain GACZR 1273 and GACOZR 1273. More impregnation of zirconium may cause the widening of the existing pores as well as the formation of large pores by additional burning of the walls between the adjacent pores during the later stages of activation.

3.2 SURFACE CHEMISTRY OF Zr4+ IMPREGNATED CARBON

Nitric acid treatment of carbons generate larger amounts of oxygen functional groups on the carbon surface. These extra surface oxygen groups on the resulted carbons are having acidic character, due to carboxylic, phenolic, and lactonic groups are determined by neutralization with a base of $NaHCO_3$, $NaOH$, and Na_2CO_3 respectively in aqueous phase. Whereas, basic groups (pyrones) are determined by neutralization with HCl. The results shown in Table 2 indicate surface modified carbon GACO has more C-O acid functional groups. It indicates that, the number of acidic sites increases when carbon is reacted with the oxidizing agent. On the other hand, the numbers of basic sites are decreased during acid oxidation modification (Pradhan & Sandle, 1999).

Figure 2(a) and Figure 2(b) shows the FTIR spectra of new activated carbon series. Relatively high intensity-peak is observed at 3460 cm⁻¹, 1640 cm⁻¹, 2919 cm⁻¹and 1100 cm⁻¹ for HNO_3 modified carbons compared to the native form GAC 383.

The peak at 3460 cm⁻¹ attributed to O-H stretching vibration of the hydroxyl group and 2919 cm⁻¹ is due to symmetric and asymmetric stretching vibration of C-H bond. The peak at 1640 cm⁻¹ is a characteristic of most carbon materials, is ascribed to the carbonyl group which is highly conjugated in the graphene layers having quinine structure C=O. The band at 1100 cm⁻¹ is ascribed as C-O stretching and O-H bending modes of alcoholic, phenolic, and carboxylic groups (Belhamdi, Merzougui, Trarib, & Addoun, 2016; Jia & Thomas, 2000; Liao, Sun, Guo, Ding, & Su, 2016; Liu et al., 2012).

XRD spectrum for GAC 383 and GACZR 1273 is given in Figure 3(a) and GACO 383 and GACOZR 1273 given in Figure 3(b). From the XRD spectrum, the interlayer spacing d_{002} is determined using the Bragg Eq.(4)

$$d = \lambda / 2sin\,\vartheta \qquad (4)$$

Where λ is the x-ray wavelength and ϑ is the scattering angle for the peak position. The crystallite size along c-axis Lc, and the size of the layer planes La, are determined from the half-width of the respective diffraction peak using the Scherrer Eq.(5)

$$L = K\lambda / B\,cos\,\vartheta \qquad (5)$$

Where L is Lc or La, B is the half-width of the peak in radians, and K is the shape factor. The quantities Lc and La are named as stack height and stack width of carbon crystallites for the new carbon respectively. The shape factor $K = 0.9$ and $K = 1.84$ are used for calculation of Lc and La, respectively (Kercher & Nagle, 2003; Zhao, Yang, Li, Yu, & Jin, 2009). The diffraction pattern had broad peaks at around 24 and 42° for the new carbon are assigned to the reflection from (002) and (100) planes, respectively. The (002) peaks are used to calculate Lc and La. The occurrence of broad peaks at 2ϑ indicated a well-defined crystal structure that resulted in better layer alignment. The interlayer spacing (d_{002}), summarized in Table 2 are in the range of 0.36 to 0.37 nm. This indicates that the granular activated carbons obtained are nongraphitized carbons.

It is known that nongraphitized carbon shows well developed microporous structure, that is preserved even during the high temperature treatment. Most activated carbons exhibit a more open structure, characteristic of highly defective carbon plates. Subsequently, smaller regions of orientational order (microscale order) are more prevalent (Thomson & Gubbins, 2000).

Morphological observation by SEM shows that, the wide ranges of pores are present on new granular activated carbon. Pores present in GACOZR 1273 are appearing more open compared to GACZR 1273 as seen in the Figure 4(a) & (b). It reveals nitric acid modification caused the widening of pores on GACOZR 1273. This carbon has relatively less N_2 adsorption; measured BET pore volume and surface area are lower than that of starting carbon GAC 383 as seen in Table 3. This is because an increase in the degree of activation makes the pore walls thin. These are more easily destroyed during the HNO$_3$ treatment, results in widening of the microporosity (Fierro, Torné-Fernández, Montané, & Celzard, 2008). TEM images illustrate (Fig. 5) the variation of the surface features due to the loading of the zirconium ions onto the GAC. In the TEM image, the presence of dark area on carbon suggests successful impregnation of zirconyl chloride onto GAC granules and the particles are randomly oriented inside the pore structure.

3.3 SOLID-GAS ADSORPTION ISOTHERMS (N₂ ISOTHERM AT 77 K)

The N_2 adsorption isotherms of the activated carbons show Type 1 isotherm as per the IUPAC classification.

It is seen in the Figure 6 that all isotherms have a steep rise in the initial stage of adsorption at lower p/p_0 range. Thereafter adsorption progressed well to attain saturation at high pressure range. Micropores are preferably filled at $p/p_0 < 0.2$ as evidenced by a distinct steep adsorption front, assigned to very high adsorption efficiency of the material within the narrow micropore range (Simões, Hoffmann, Claudio, & Wilhelm, 2016).

The pore volume and the respective specific surface area of each carbon have been determined for predicting the efficiency of the material. In this regard, a series of isotherm analysis applied. BET, I plot, Langmuir, Freundlich, and Dubinin- Radushkevich (D-R) methods were followed using N_2 adsorption data at 77K.

3.3.1 Brunauer Emmett Teller (BET) Isotherm Analysis

The BET isotherm method based on a theory of multilayer adsorption was applied for the carbons and the respective BET surface area was calculated from the isotherm using Eq. (6)

$$\frac{1}{V(\frac{p_0}{P}-1)} = \frac{1}{V_m C} + \frac{C-1}{V_m C}\left(\frac{p}{p_0}\right) \qquad (6)$$

A plot of $\frac{1}{V(\frac{p_0}{P}-1)}$ verses $\left(\frac{p}{p_0}\right)$ for each carbon gives a straight line with slope $\frac{C-1}{V_m C}$ and intercept $\frac{1}{V_m C}$. Accordingly, the monolayer volume V_m and the constant C are calculated. The linear plot, is extended in the range $0.05 < P < 0.3$ for the respective BET analysis. From the isotherm constant V_m calculated the specific surface area using Eq. (7)

$$SA_{BET} = \frac{V_m(Cm^3/g) \times 6.023 \times 10^{23} \times 0.162 \times 10^{-18}(m^2/N_2 molecule)}{22414(cm^3/mol)} \qquad (7)$$

Table 3 shows the results of BET analysis for the new carbons. Here some discrepancy due to lack of a positive C character is observed for the BET equation in the region $0.05 < P < 0.3$. The negative value of C has no significant meaning. For ideal microporous materials, C_{BET} is usually positive and it has to be greater than 150. This shows the multilayer adsorption on the new carbons is not fully following the BET model. BET analysis of the adsorption data for the relative pressure range p/p_0 up to 0.1 make C_{BET} become positive. Here, the condition for C_{BET} value greater than 150 is satisfied in all cases (Fig.7).

Furthermore, it is known that C in Eq. (6) is not actually a constant but a parameter, is given by the relation $C = exp(q_1 - q_L)/RT$. The determination of C parameter in the whole range of adsorption is unattainable. Also, the linear part of the traditional BET plot $(0.05 < P < 0.3)$ is not well defined. So there are many ambiguities in the determination of V_m and specific surface area (SA) by BET method, particularly with respect to microporous materials (Sing, 2001).

3.3.2 I-Point method Analysis

The rearrangement of the BET equation in Scatchard-type form, provide the isotherm line with slope equal to $(C-1)$ at any p/p_0 and V. This plot is known as BET-Scatchard (B-S) plot (Pomonis et al., 2005) given by Eq. (8)

$$[V(1 - \tfrac{p}{p_0})]/\tfrac{p}{p_0} = CV_m - (C-1)[V(1 - \tfrac{p}{p_o})] \qquad (8)$$

The graphs (Fig. 8) give an inclined V shape curve (⌄) with an inversion point termed I point. The extrapolation of this point towards x-axis ismarked and taken as V_m i.e. $[V (1-P)]_{I\ point} = V_m$ (monolayer volume of I plot method) (Collins et al 2011). V_m can be used for the determination of surface area. Specific surface area is calculated using Eq. (9)

$$SA = 4.356V_m. \qquad (9)$$

Hence the I point method provides an alternate way to determine the surface area of new carbons without any ambiguities. Mostly, these carbons have a C parameter (BET) positive for further plotting of N_2 data at $p/p_0 < 0.1$ and simultaneously fitting the BET model for confirmation. The surface area was calculated from the monolayer volume $[V_m = V_I(1 - \tfrac{p}{p_o})]$.

On BET analysis of isotherm data up to $p/p_0 = 0.1$ has resulted comparable surface area similar to that obtained from I plot. The critical evaluation of isotherm constants by the BET and I-plot method revealed that the materials are convincingly microporous with pore width ranges 1.71 - 1.77 nm. The average pore width of carbon calculated using the Eq. (10)

$$d = 4V_T/SA_{BET} \qquad (10)$$

The major factors governing the selectivity of active carbons is the pore characteristics, i.e. pore size distribution and pore volume (Branton & Bradley, 2011).

In this regard, pore volume, pore width and surface area of new carbons are shown in Table 3.

BET surface area of the carbon activated and impregnated with Zr^{4+} has been 1497.3 m²/g for the pore volume of 0.640 cm³/g while, that for GAC 383 was 1298.5 m²/g for the pore volume 0.573 cm³/g. The significance of this study is that Zr^{4+} activation enhanced the total pore volume, micropore volume and specific surface area of GAC.

The monolayer-multilayer adsorption appears to happen as a cooperative micropore filling at high p/p_0 prior to capillary condensation. This allows to apply a series of isotherm models for the evaluation of monolayer volume valid for a Type I (Langmuir type) isotherm.
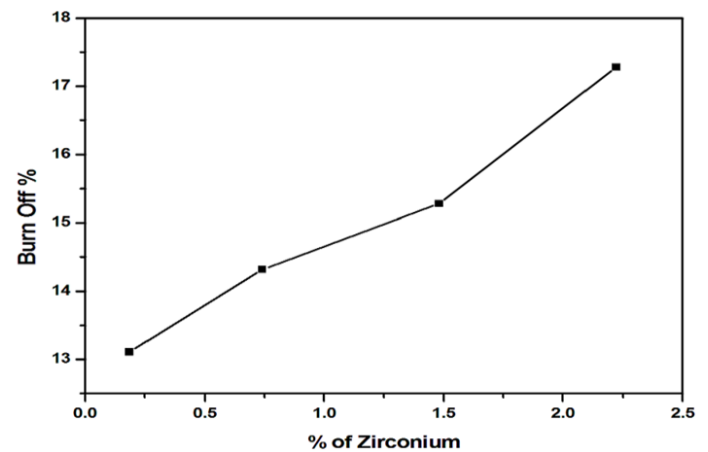

Fig. 1. Plot of burnoff vs % of zirconium ion impregnated.

Table 1. Effect of zirconyl chloride on carbon yield and burn off.

Amount of (ZrOCl₂.8H₂O)	% of zirconium in carbon	Carbon yield%	Burn off%
0.065	0.2	86.89	13.11
0.26	0.7	85.68	14.32
0.52	1.5	84.72	15.28
0.78	2.2	82.72	17.28

3.3.3 Langmuir Isotherm Analysis

Langmuir equation (Langmuir, 1918) is applied to the new carbons to study monolayer adsorption behaviour. The general form used to plot N_2 isotherm at 77K is given by Eq. (11)

$$\frac{P}{V} = \frac{1}{bV_m} + \frac{P}{V_m} \qquad (11)$$

$P = \frac{p}{p_0}$, where, p is equilibrium vapour pressure, p_0 is the saturation vapour pressure and V_m is monolayer adsorption capacity (mmol/g). From the graph of P/V verses P, a straight line is obtained and from the slope and intercept, V_m (monolayer volume) and constant b are calculated. As per the IUPAC (2015), most Type 1 isotherms corresponds to the so-called Langmuirian isotherms. In the case of physical adsorption, the Type 1 isotherm represents the presence of micropores, where molecules are adsorbed by micropore filling (Kaneko, 1994). The resulting Langmuir isotherms have perfect linearity (0.999) for all GACs as shown in the Figure 9(a). The Zr^{4+} impregnated carbon GACZR 1273 has relatively high monolayer capacity ($V_m = 388\ cm^3/g$) and hence specific surface area ($1687\ m^2/g$). This indicates that the monolayer coverage of the carbon was associated with so-called micropore filling. Surface area obtained from Langmuir and BET methods shown difference of 12-13%. This reveals that the monolayer capacity and the corresponding surface area does not reflect exact surface area, rather than an equivalent or characteristic surface area (Lowell & Shields, 1991). The nature of the physical interaction of N_2 if any exists in the new carbon materials have to be revealed on applying Freundlich isotherm model.
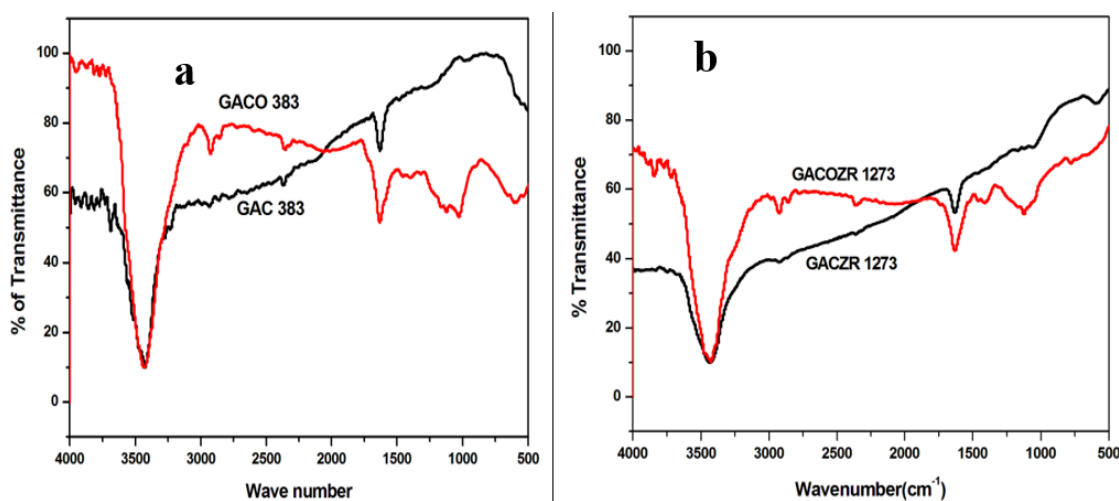

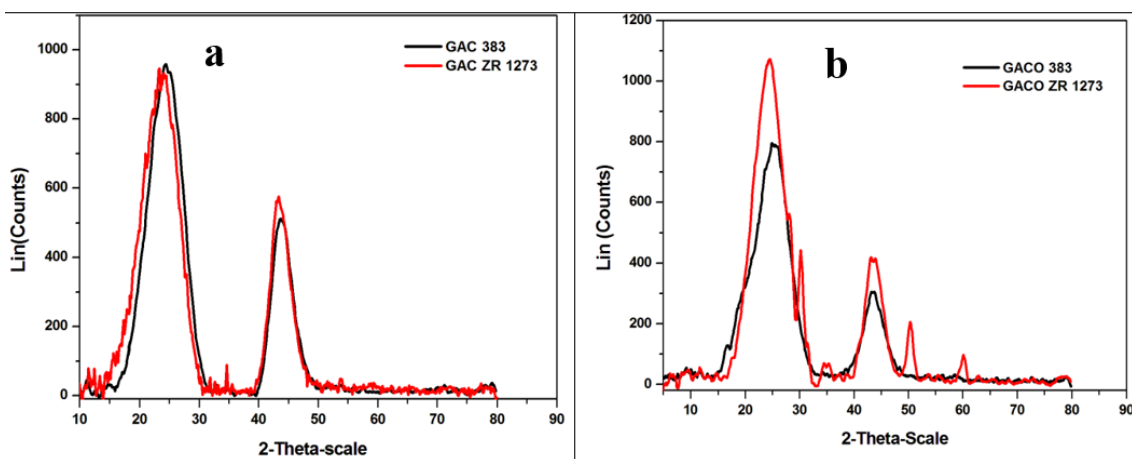Fig. 2. FTIR spectra of (a) GAC 383, GACO 383 and (b) GACZR1273 and GACOZR 1273.

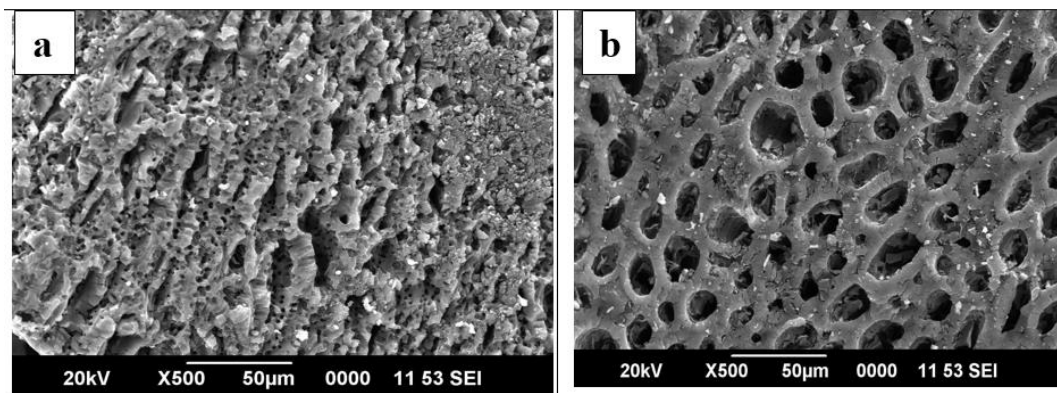Fig. 3. XRD spectra of (a) GAC 383, GACZR 1273 and (b) XRD spectra of GACO 383, GACOZR 1273.

Fig. 4. SEM images of carbon (a) GACZR 1273 and (b) nitric acid modified form of carbon GACOZR 1273.

Table 2. Surface oxygen functional groups by Boehm titration and
Crystalline parameters by XRD.

Sample name	Surface functional group				XRD parameters		
	Carboxylic meq/g	Phenolic meq/g	Lactonic meq/g	Base meq/g	Lc (0.9)	La (1.84)	d_{002}
GAC 383	0.40	0.45	0.18	0.50	1.14	2.28	0.36
GACO 383	1.38	2.10	1.34	0.20	0.97	1.94	0.36
GACZR 1273	0.39	0.44	0.20	0.62	0.98	2.00	0.37
GACOZR 1273	0.62	1.52	0.90	0.38	1.31	2.68	0.36

Table 3. Porosity parameters calculated from nitrogen adsorption isotherms (N2 /77K) using BET and
I plot methods.

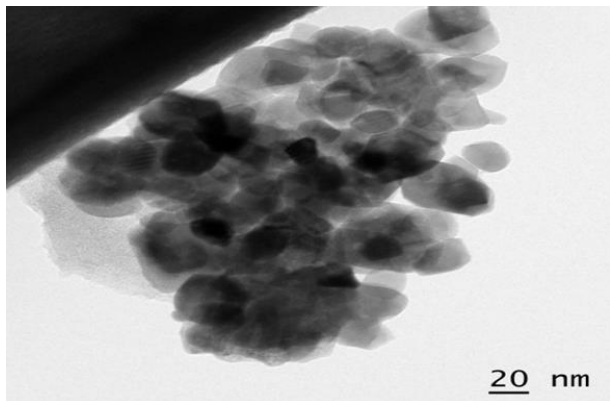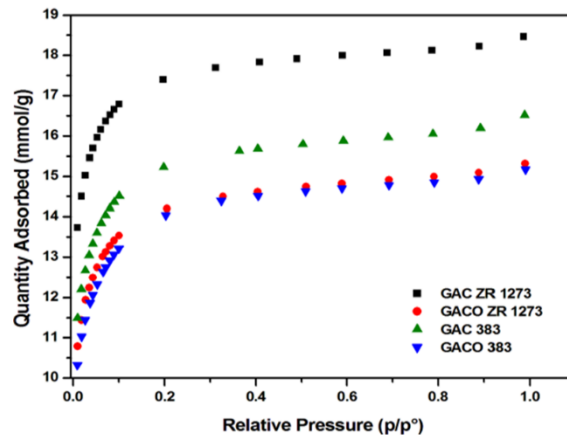| Sample	Total Pore volume cm³/g	BET Analysis (p/p₀ upto 0.3)			I plot		BET Analysis (p/p₀ upto 0.1)			
		SA_{BET} m²/g	V_m cm³/g STP	C_{BET}	S_I m²/g	$V_m = V_I$ cm³/g STP	SA_{BET} m²/g	V_m cm³/g STP	C_{BET}	Pore width (nm)
GAC 383	0.573	996.8	229	-81.6	1275.4	293	1298.5	298.3	524	1.76
GACO 383	0.526	974.3	224	-119	1164.6	267.5	1186.5	272.5	439	1.77
GACZR 1273	0.640	1217.2	280	-104	1482.1	340.5	1497.3	343.9	873	1.71
GACOZR1273	0.531	976.2	224	-103	1193.2	274.1	1212.2	278.5	563	1.75

Fig. 5. TEM images of GACZR 1273.

Fig. 6. N_2 adsorption isotherm plot for the new carbons at 77K.
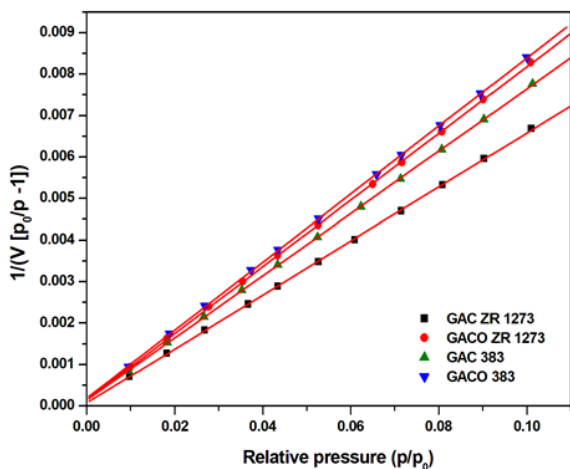

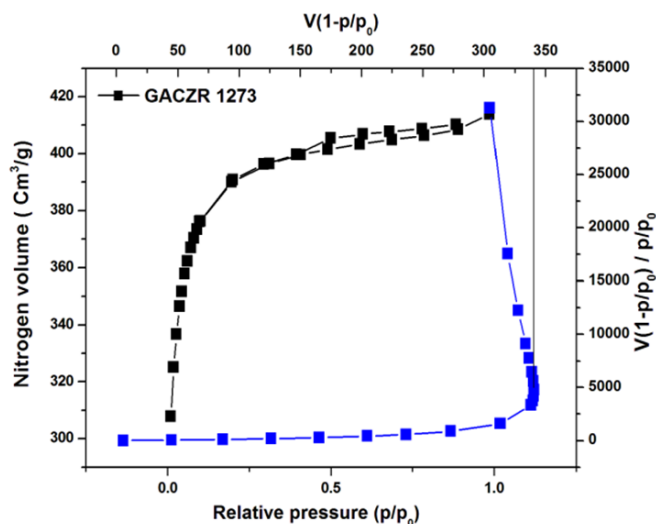Fig. 7. BET isotherm plot for the new carbons at 77K.

Fig. 8. I plot method for the new carbons at 77K.

3.3.4 Freundlich Isotherm Analysis

Physisorption of N_2 gas on the carbons was evaluated using the Freundlich isotherm equation by the relationship as per Eq. (12) (Achari, 1998; Kumar, de Castro, Martinez-Escandell, Molina-Sabio, & Rodriguez-Reinoso, 2010).

$$\log V = \log K_F + \frac{1}{n} \log P \qquad (12)$$

A plot of *log V* verses *log P* gives a straight line with intercept *log K_F* and slope *1/n* as given in Figure 9(b). All the carbons have straight line graphs with the correlation coefficient $R^2 = 0.999$ revealed a strong interaction between the carbon and nitrogen gas at 77K. It is known

that Freundlich "*n*" value is a measure of adsorption intensity for physisorption mechanism to occur and it ranges from 9.4 -11.5 for the carbon studied . The modified carbon GACZR 1273 shows the highest '*n*' (11.5) and K_F (259) compared to others (Table 4).

The isotherm behaviour and porosity development of the new carbon have been further evaluated, applying the Dubinin-Radushkevich (D-R) isotherm model.

3.3.5 Dubinin-Radushkevich (D-R) Isotherm Analysis

Dubinin-Radushkevich (D-R) equation (Dubinin, 1960; Dubinin & Kadlec, 1975) is used to determine micropore volume of the new carbons from the N_2

adsorption isotherm at 77K. A plot of *log W* verses $log^2 \left(\frac{p}{p_0}\right)$ gives linearity in the low pressure region, *(p/p₀ < 0.1)* i.e. where the narrow micropores are filled as shown in the Figure 9(c).

$$\log W = \log W_0 - D log^2 \left(\frac{p}{p0}\right) \qquad (13)$$

W is the amount (mmol) of *N₂* gas gets filled in micropore of carbons. The parameters, characterization energy *(E₀)*, pore width *(L)*, and micropore surface area *(SA_{D-R})* are calculated and given in Table 4. *E₀* is related to pore width *L* as per the Eq. (14)

$$L = \frac{10.8}{(E_0 - 11.4)} nm \qquad (14)$$

$$SA_{D-R} = \frac{2 \times 10^3 \times W_0 (cm^3/g)}{L} \qquad (15)$$

The carbon obtained by incorporating *Zr⁴⁺* has an *L* value between 1.92 - 2.48 nm i.e the micropore surface area was contributed mainly by pores less than 2.0 nm that are very much generated by *Zr⁴⁺* ions during chemical activation.

Dubinin-Radushkevich (D-R) isotherm analysis shows that GACZR 1273 has much higher micropore volume (401.7cm³/g) and micropore surface area (648 m²/g) as compared to that of basic carbon GAC 383 (micropore volume of 351.3 cm³/g and surface area, 425 m²/g). This indicates that carbon has extra porosity due to *Zr⁴⁺* activation and the energy of adsorption *(E₀)* is 15-17 k J/mol, common for the physical nature of adsorption in pores having width < 2.0 nm.
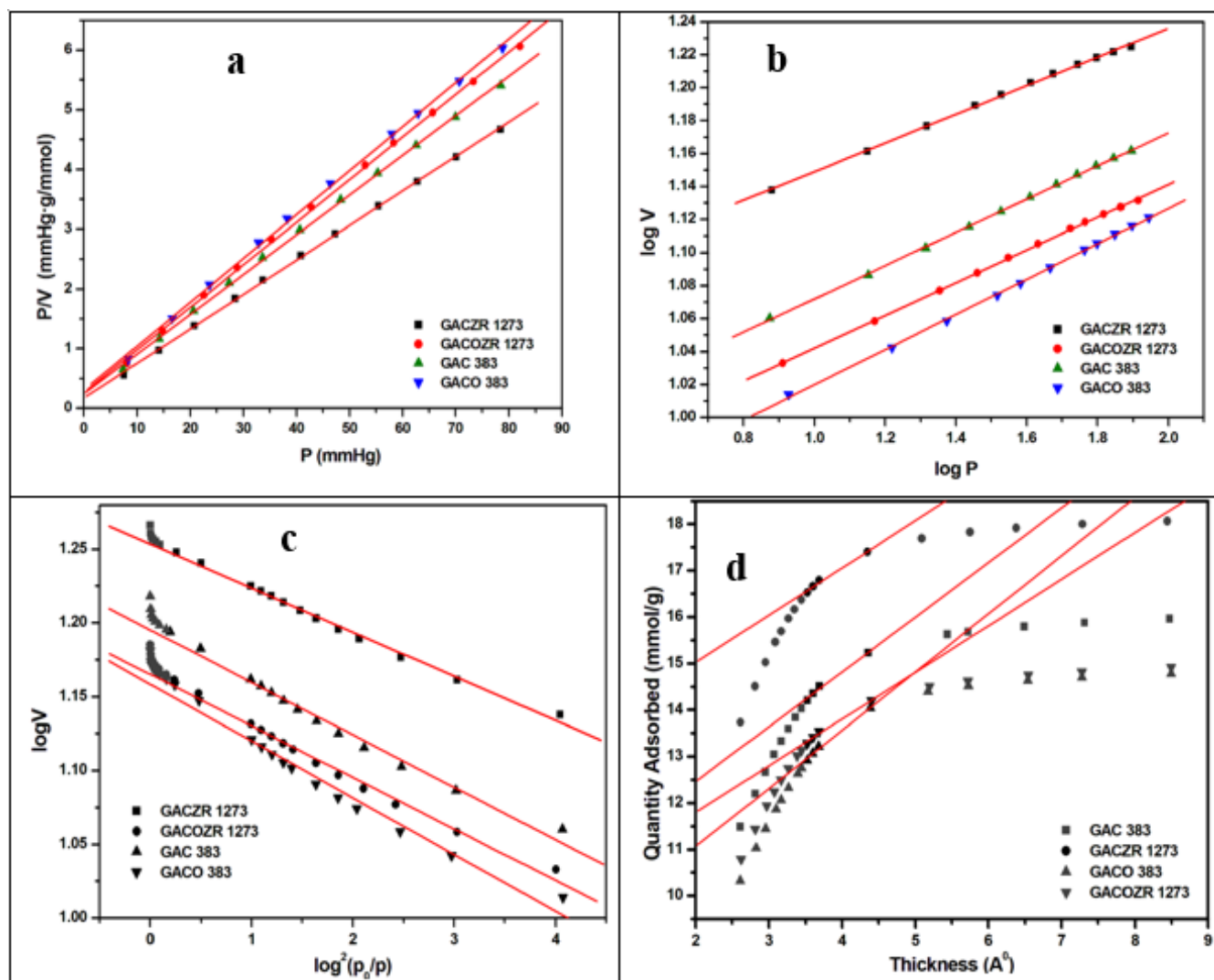

Fig. 9. (a) Langmuir, and (b) Freundlich, (c) Dubinin-Radushkevich (D-R) isotherm and (d) t plots of GAC 383, GACO 383 and GACZR 1273 and GACOZR 1273 using N2 adsorption data.

Table 4. Porosity parameters calculated from nitrogen adsorption N_2/77K using Langmuir, Freundlich, & Dubinin-Radushkevich isotherms.

Sample	Langmuir			Freundlich			D-R				
	SA_L m²/g	V_m cm³ /g	R^2	n	K_F	R^2	SA_{D-R} m²/g	W_o cm³/g	L nm	E kJ/ mol	R^2
GAC 383	1465	337	0.99	9.4	210	0.99	424.7	351.3	2.56	15.6	0.98
GACO 383	1326	304	0.99	9.4	184	0.99	334.1	322.8	2.99	15.0	0.98
GACZR 1273	1687	388	0.99	11.5	259	0.99	647.9	401.7	1.92	17.0	0.99
GACOZR1273	1367	314	0.99	10.1	196	0.99	409.4	327.8	2.48	15.8	0.99

3.3.6 t-plot method

Lippens and de Boer (Lippens & de Boer, 1964; Lippens, Linsen, & de Boer, 1964) proposed 't' plot method for the determination of micropore volume and external surface area by plotting the thickness of adsorbed layer t against the amount adsorbed as shown in the Figure 9 (d). This isotherm is specific to determine micropore and mesopore filling. The external surface area (SA_{ext}), micro pore surface area (SA_{mic}), and micropore volume (V_{mi}) are given in Table 5. The GAC has the distinct steep rise with respect to quantity adsorbed (mmol/g) in 't' plot in the initial range of adsorbed thickness, to attain maximum with a. round knee. Finally become oriented slightly parallel to x-axis at the higher ranges of adsorbed thickness. A straight line is drawn in the linear region of the t plot. From the slope and intercept the external surface area (SA $_{ext}$) and micropore volume (V_{mi}) are calculated.

$$t = [13.99/(0.034 - \log(^p/_{p_0}))] \qquad (16)$$

Where t is the thickness of the pores and p/p_0 is the relative pressure.
External surface area,

$$SA_{ext} = \frac{slope \times (10^{10} A^0/m) \times D}{F \times 10^6} \qquad (17)$$

Where D is the density conversion factor = 0.0015468. F = surface area correction factor, for most samples it is taken as 1.0.
Micropore volume, V_{mi} (cm³ /g), can be calculated by multiplying *intercept* obtained from the t plot with density conversion factor D, given in Eq. (18).

$$V_{mi} = intercept \ (cm^3 \ /g \ STP) \times D \qquad (18)$$

Micropore surface area $SA_{mi}(m^2/g) = SA_{BET} - SA_{ext} \qquad (19)$

Where SA_{BET} is the BET surface area and SA_{ext} is the external surface area.

High external surface area of GACO 383 indicates that nitric acid modified carbon possesses a significant amount of larger pores. This is evidenced by the external surface area up to 6.28 % more compared to basic carbon GAC 383. This is caused by the reduction of micropore volume up to 15.32 % due to the widening of existing micropores. Activation of carbon GAC 383 with Zr^{4+} (GACZR 1273) enhances the micropore volume up to 28.40 %, indicate that the activated carbon GACZR 1273 produced is predominantly consists of micropores. In fact, of the total surface area of this carbon (S_T), micropore surface area contributes 70.0 % and only the remaining 30.0 % contribute external surface area. Means, Zr^{4+} activation leads to the acceleration of porosity development on the activated carbon matrix of GAC 383. It is seen that Zr^{4+} activated nitric acid modified carbon GACOZR 1273 has a less proportion of micropores. This is evidenced by a 24.56 % decrease in micropore volume compared to GACZR 1273. Simultaneously, there is no increase in the external surface area, because the extent of pore widening in GACOZR 1273 is relatively less.

3.3.7 BJH (Barrett Joyner Halenda) method

Pore size distribution of GAC series has been done based on SA_{BET}, V_{mi}, V_{ext} and adsorption average pore width from

the N_2 adsorption data at 77 K. The pore size distribution is a measure of physical characteristics of carbon (porous) materials to predict the extent of pore accessibility of an adsorbate molecule. The pore size distribution was determined by the BJH (*Barrett Joyner Halenda*) method. Distribution curves of pore volume and specific surface area are described as a function of pore width (A^0) drawn from the N_2 adsorption-desorption data. The adsorption cumulative surface area (ADSCA), desorption cumulative surface area (DCSA), respective pore volumes (ACPV and DCPV) and pore width (ads and des) are computed, given in Table 5.

The BJH pore size distribution shows the new carbons are having pore width in the range 2.0-2.24 nm. This supports the evidence for the existence of the fractional mesoporosity (Bindia, 2016).

Table 5. Porosity parameters calculated from nitrogen adsorption isotherms at 77K using t-plot & BJH method.

Sample	t-plot			BJH					
	V_{mi} cm^3/g	SA_{mi} m^2/g	SA_{ext} m^2/g	ADCSA m^2/g	DCSA m^2/g	ACPV cm^3/g	DCPV cm^3/g	Pore width (ads) A^0	Pore width (des) A^0
GAC 383	226.70	588.65	408.10	226.21	220.52	0.138	0.134	24.35	24.30
GACO 383	191.96	540.28	433.72	250.00	242.84	0.142	0.137	22.78	22.55
GACZR 1273	291.07	863.84	353.40	196.07	207.50	0.117	0.121	23.89	23.22
GACOZR 1273	219.58	628.45	347.80	204.04	205.76	0.123	0.123	24.10	23.86

3.4 SOLID-LIQUID ADSORPTION ISOTHERM STUDY: PHENOL

Adsorption characteristics of all carbons for the removal of phenol are shown in the Figure 10. Equilibrium adsorption isotherm studies show that the adsorption increases with phenol concentration. Adsorption data are fitted to well-known models of Langmuir, Freundlich, and Dubinin-Radushkevich (D-R) isotherms. Adsorptive capacity of Zr^{4+} impregnated coconut shell based granular carbon is relatively high. Among this group studied, oxidized carbon GACO 383 has less adsorption capacity than others. This is because, a higher proportion of carbon- oxygen surface functional groups (mainly COOH) ionize in water to produce H^+ ions. The resulting COO- directed towards liquid phase bear negative charges on the carbon surface hence suppresses the further adsorption of phenol. Langmuir, Freundlich and D-R isotherm parameters were determined and presented in Table 6.

3.4.1 Langmuir isotherm:

The Langmuir isotherm is prominent to describe a homogeneous adsorption system in liquid phase where each molecule adsorbed onto the surface has uniform adsorption energy. Linear form of Langmuir isotherm model is used to evaluate phenol adsorption behaviour of new carbons. (Achari & Jayasree, 2014; Achari & Rajalakshmi, 2014)

$$\frac{C_e}{q_e} = \frac{1}{K_L} + \frac{a_L}{K_L} C_e \qquad (20)$$

Where C_e and q_e are the phenol concentration in the liquid phase and solid phase respectively at equilibrium. K_L and a_L are the Langmuir constants, K_L/a_L ($=q_m$) is known as monolayer adsorption capacity. The parameter q_m and K_L are determined by plotting C_e versus $\frac{C_e}{q_e}$. Langmuir isotherm assumes that, monolayer adsorption takes place

onto the solid surface (carbon) containing a finite number of adsorption sites having uniform adsorption energies, without transmigration of the adsorbate (phenol) in the plane of the adsorbent surface. Langmuir isotherm plot for carbons GAC 383, GACO 383, GACZR 1273 and GACOZR 1273 is shown in the Figure 11. Isotherms show the Type I features of uniform microporosity for all carbons.

3.4.2 Freundlich isotherm:

Freundlich isotherm model commonly used to describe the adsorption characteristic of heterogeneous surfaces is applied to the new carbon – phenol adsorption system. Figure 12 represents the Freundlich isotherm plots of phenol adsorbed by unit mass of carbon. The linear form of the equation applied is given as follows (Ma, Zhu, Xi, Zhu, & He, 2016).

$$log q_e = log K_F + \frac{1}{n} log C_e \qquad (21)$$

Where C_e and q_e are the liquid phase phenol concentration (mg/L) and solid phase concentration (mg/g) respectively at equilibrium. K_F is a function of the energy of adsorption as well as a measure of adsorptive capacity. $1/n$ determines the intensity of adsorption. As regards to new carbon series, K_F and n are evaluated and given in Table 6.

3.4.3 Dubinin-Radushkevich (D-R) isotherm:

The D-R isotherm generally applied to express the adsorption mechanism with a Gaussian energy distribution onto a heterogeneous surface specifically for gas-solid equilibria. In the case of liquid-phase adsorption Dubinin-Radushkevich (D-R) equation assumes that, the adsorption occurs in micropores and is limited to a monolayer. The linear form of D-R equation is expressed as

$$ln q_e = ln q_{mi} - \beta \varepsilon^2 \qquad (22)$$

β is a constant related to the energy of adsorption, ε is the Dubinin-Radushkevich isotherm constant and q_{mi} is a measure of adsorption capacity.

Where $\varepsilon = RTln[1 + \frac{1}{C_e}]$ (23)

D-R isotherm is plotted as a function of the logarithm of amount adsorbed ($ln\ q_e$) versus ε^2 (Fig. 13).

The mean free energy, E per molecule of adsorbate (for removing a molecule from its location in the sorption space to the infinity) can be determined by the Eq.(24) (Dada, Olalekan, Olatunya, & Dada, 2012; Stoeckli et al., 2001).

$$E = \frac{1}{\sqrt{2\beta}} \qquad (24)$$

Regarding the isotherm analysis, equilibrium data for phenol adsorption were well fitted to the Langmuir model with monolayer adsorption capacity of GACZR 1273 (342.5 mg/g), GAC 383 (312.5 mg/g) for GACOZR 1273 (280.9 mg/g) and GACO 383 (209 mg/g). From the Table 6 it is clear that, the interaction of phenol on the GACZR 1273 is prominent due to chemical activation with zirconium (Zr^{4+}) ions. At the same time nitric acid modification of carbon decreased the adsorption efficiency of GACO 383 and GACOZR 1273 towards phenol.

Adsorption analysis of phenol using Freundlich finds that constant K_F (adsorption binding constant) varies in the range of 16.7 - 33.8, and n (adsorption intensity) is in the range of 2.49 - 3.12, confirms favourable adsorption as it lies between 1-10.

Dubinin-Radushkevich parameters q_m and β are determined from the intercept and slope of isotherm plot and are given in Table 6. The adsorbed amount (q_{mi}) is 69.2 mg/g for Zr^{4+} modified carbon GACZR 1273. It indicates that micropores are developed on GAC 383 during activation after impregnation with Zr^{4+} are accessible in solid-liquid adsorption equilibria. Dubinin-Radushkevich adsorption isotherm analysis of solid-gas equilibria of N_2 at 77K [Table 4] substantiate the formation and contribution of enough micropores (hence evaluation of micropore volume) towards specific surface area. The result reveals that GACZR 1273 has micropore surface area SA_{D-R} of 647.9 m^2/g, whereas the native carbon GAC 383 has SA $_{D-R}$ of 424.7 m^2/g only. This means Zr^{4+} ions promoted an extra microporosity of 223.2 m^2/g. This is further confirmed by the results of $t-$ plot analysis (Table 5), which reveals SA $_{mi}$ is 863.8 m^2/g for GACZR 1273, whereas SA $_{mi}$ is 588.65 m^2/g for GAC 383. Extra porosity due to Zr^{4+} activation promotes higher phenol adsorption efficiency for the carbons. The mean free energy E calculated is in the range of 0.292 - 0.896 kJ/mol shows phenol adsorption follows physisorption process, i.e. adsorbate is bound to the surface of the carbons by relatively weak Van der Waals forces.

Nitric acid modified carbon GACO 383, and its zirconium (Zr^{4+}) activated form GACOZR 1273 has a less adsorption efficiency compared to GAC 383 and GACZR 1273 (Table 6). More acidic groups already occupied on the carbon surface make them unfavourable and inacceassible for the approach of phenol molecule. Because, it reduces the electron density on the basal plane of the carbon. This further reduces the $\pi - \pi*$ interaction between the phenol aromatic ring and the basal plane of the carbon. Also, surface acidic functional group COOH ionizes and exist as negative sites (-COO⁻) on the carbon surface. It repels the incoming phenoxide ions reducing the extent of donor-acceptor interaction between the phenolic group and carbon surface (Vinod & Anirudhan, 2002).

Fig. 10. Adsorption isotherm of phenol on GAC 383, GACO 383, GACZR 1273 and GACOZR 1273.
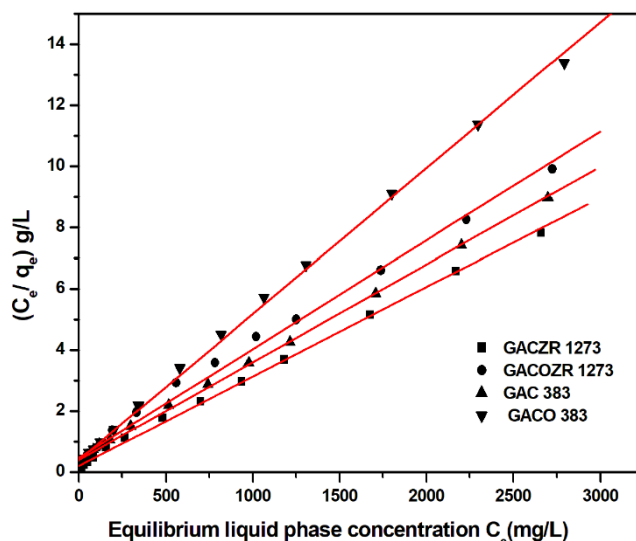

Fig. 11. Langmuir Adsorption isotherm of phenol on GAC 383, GACO 383, GACZR 1273 and GACOZR 1273.
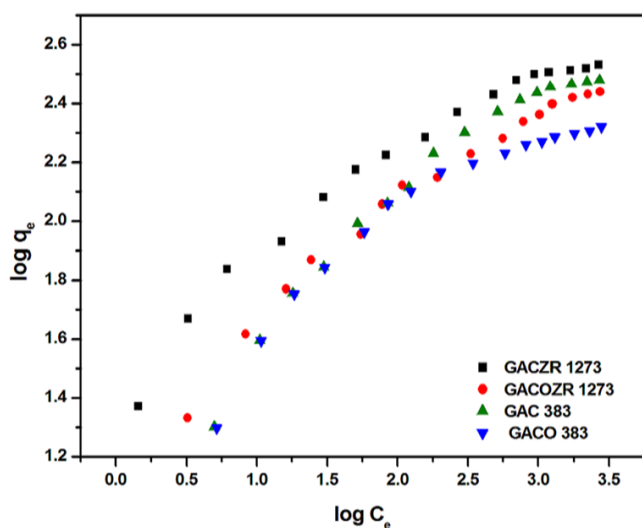

Fig. 12. Freundlich Adsorption isotherm of phenol on GAC 383, GACO 383, GACZR 1273 and GACOZR 1273.
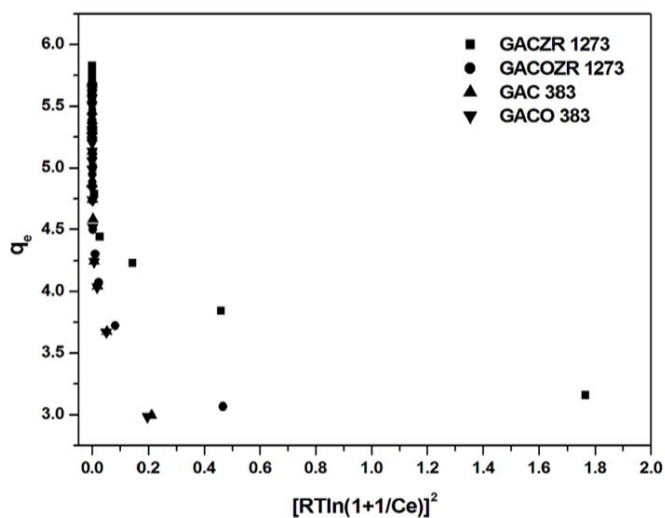

Fig. 13. Dubinin-Radushkevich Adsorption Isotherm of phenol on GAC 383, GACO 383, GACZR 1273 and GACOZR 1273.

Table 6. Adsorption parameters of phenol on GAC obtained from Langmuir, Freundlich and Dubinin- Radushkevich isotherm at 300C.

Sample	Langmuir isotherm parameter			Freundlich isotherm parameter			D-R isotherm parameter			
	q_m	K_L	R	n	K_F	R	q_{mi}	β	R	E
	(mg/g)	L/mg			L/g		mg/g			k J/mol
GAC 383K	312.50	2.48	0.999	2.49	16.73	0.972	57.38	5. 08	0.983	0.293
GACO383K	209.64	2.48	0.999	3.12	20.71	0.945	57.41	5.50	0.985	0.302
GACZR 1273	342.47	4.83	0.999	3.10	33.85	0.973	69.21	0.622	0.984	0.897
GACOZR 1273	280.90	2.11	0.997	2.87	20.99	0.981	55.51	2.07	0.974	0.492

4. CONCLUSION

Chemical activation of GAC with $ZrOCl_2.8H_2O$ brought marked changes in the burn off, pore development, and carbon yield. The nitric acid oxidation of GAC 383 causes changes in the microcrystallinity of the carbon layers as evidenced by distinct changes *in La, Lc* and d_{002} values. The nitric acid treatment enhances the proportion of surface oxygen groups on carbon surface. Surface morphological studies using SEM indicate that carbon has a uniform and well developed porous structure. HNO_3 acid treatment destroys the nature of thin pore walls existed on GAC 383 surface that leads to the widening of micropores. Activating agent Zr^{4+}ions are randomly distributed deep inside the GAC as evidenced by TEM profile. All the four carbons studied shows Type I isotherm character as per IUPAC classification. The critical evaluation of isotherms and constants by BET and *t*-plot method revealed that the carbons (GAC 383, GACO 383, GACZR 1273 and GACOZR 1273) are convincingly microporous with average pore width ranges 1.71-1.77 nm. Langmuir and Dubinin-Radushkevich isotherm analysis established that pore volume and specific surface area of zirconium impregnated carbon GACZR 1273 is significantly higher than the native carbons GAC 383 and its prodigy GACO 383. The *t*-plot Analysis showed that of the total surface area of GACZR 1273 (1217.24 m²/g) only 30% (353.40 m²/g) is contributed by external surface area. This suggests that 70% (863.84 m²/g) of the total surface area is truly contributed by the micropores. Hence Zr^{4+}activation promotes extra microporosity on the coconut shell based granular activated carbon. Pore size distribution (PSD) showed that the adsorption pore diameter is in ranges 2.28 - 2.43 nm, and desorption pore width ranges 2.25 - 2.43 nm for the group of activated carbons studied. HNO_3 oxidized carbon (GACO 383) has relatively less affinity for the adsorption of phenol. Carbon impregnated and activated with Zr^{4+} (GACZR 1273) has a higher phenol uptake capacity (342.5 mg/g). From these observations, it is concluded that higher adsorption performance of the new Zr^{4+} incorporated carbons are due to the formation of more open pore structures with greater proportions of well defined micropores (< 2 nm), developed during chemical activation.

CONFLICT OF INTEREST

The authors have no conflicts of interest to declare.

REFERENCES

Achari, V. S. (1998). *Ph D Thesis: Modified Carbons and Wood dust Evaluation of Adsorption properties*. University of Kerala. Retrieved from Shodhganga a reservoir of Indian Thesis. http://hdl.handle.net/10603/120409

Achari, V.S., & Anirudhan, T.S.(1995). Phenol removal from aqueous systems by sorption on jackwood sawdust. *Indian journal of Chemical Technology*, 2, 137- 141. http://nopr.niscair.res.in/handle/123456789/31110

Achari, V.S., & Jayasree, S. (2014). Adsorption of nitrophenol on Zn²⁺ Impregnated Activated Carbons. In *Jayaprakash R (Edr): Learning and Dissemination of Science and Technology through Malayalam*. Paper presented at the Proceedings of the 24th Swadeshi Science Congress (India), Malappuram, Kerala (pp. 328-333). Kochi: Swadeshi science movement. ISBN: 978-81-928129-2-2.

Achari, V.S., & Rajalakshmi, A. S. (2014). Adsorption of Phenol using Zr⁴⁺ Impregnated Activated Carbon: Equilibrium and Kinetic Study. In *Jayaprakash R (Edr): Learning and Dissemination of Science and Technology Through Malayalam*. Paper presented at the Proceedings of the 24th Swadeshi Science Congress (India), Malappuram, Kerala (pp. 314-319). Kochi: Swadeshi science movement. ISBN: 978-81-928129-2-2.

Belhamdi, B., Merzougui, Z., Trarib, M., & Addoun, A. (2016). A Kinetic equilibrium and Thermodynamics study of L-phenylalanine adsorption using activated carbon based on agricultural waste (date stone), *Journal of applied research and Technology*, 14, 354-366. https://doi.org/10.1016/j.jart.2016.08.004

Bindia, R. (2016). *Ph D Thesis: Adsorption Isotherm Studies on Activated Carbon Prepared by Activation with Cerium Compounds* (Unpublished). Cochin University of Science and Technology, Cochin, India.

Branton, P., & Bradley, R. H. (2011). Effects of active carbon pore size distributions on adsorption of toxic organic compounds. *Adsorption*, *17*(2), 293–301. http://doi.org/10.1007/s10450-010-9284-4

Collins, K.E., Collins, C.H., Maroneze, C.M., Cappovila, V., & Custodio, R. (2011). Evaluations of the BET, I-point, and α-plot procedures for the routine determination of external specific surface areas of highly dispersed and porous silicas. *Langmuir*, 27(1), 187–195. http://doi.org/10.1021/la103640z

Dada, A., Olalekan, A., Olatunya, A., & Dada, O. (2012). Langmuir, Freundlich, Temkin and Dubinin – Radushkevich Isotherms Studies of Equilibrium Sorption of Zn ²⁺ Unto Phosphoric Acid Modified Rice Husk. *IOSR Journal of Applied Chemistry*, *3*(1), 38–45. http://doi.org/10.9790/5736-0313845

Dubinin, M. M. (1960). The Potential Theory of Adsorption of Gases and Vapors for adsorbents with energetically non-uniform surface. *Chemical Reviews*, 60, 35-41.

Dubinin, M. M., & Kadlec, O. (1975). New Ways in Determination of the Parameters of Porous Structure of Microporous. *Carbon*, *13*, 263–265. https://doi.org/10.1016/0008-6223(75)90026-3

EPA. (2002). *Manual Report for List of Chemical Priority*. USA: Environmental Protection Agency.

Fierro, V., Torné-Fernández, V., Montané, D., & Celzard, A. (2008). Adsorption of phenol onto activated carbons having different textural and surface properties. *Microporous and Mesoporous Materials*, 111(1-3), 276–284. http://doi.org/10.1016/j.micromeso.2007.08.002

Gebresemati. M., Gabbiye. N., & Sahu. O. (2017). Sorption of cyanide from aqueous medium by coffee husk: Response surface methodology, *Journal of applied research and Technology*, 15, 27-35. https://doi.org/10.1016/j.jart.2016.11.002

Girish, C., & Murty, V. (2012). Adsorption of phenol from wastewater using locally available adsorbents. *Journal of Environmental Research and Development*. 6 (3), 763-772. http://eprints.manipal.edu/id/eprint/137329

Hameeda, B.H., Din, A. T. M., & Ahmad, A. L. (2007). Adsorption of methylene blue onto bamboo-based activated carbon: Kinetics and equilibrium studies. *Journal of Hazardous Materials*, *141*(3), 819–825. http://doi.org/10.1016/j.jhazmat.2006.07.049

Holmes, H.F., Fuller, E.L., & Gammage, R.B.(1972). Heats of Immersion in the Zirconium Oxid-Water System. *The Journal of Physical Chemistry*, 76 (10), 1497–1502. http://doi.org/10.1021/j100654a023

Jia, Y.F., & Thomas, K. M. (2000). Adsorption of cadmium ions on oxygen surface sites in activated carbon. *Langmuir*, 16 (3), 1114–1122. http://doi.org/10.1021/la990436w

Kaneko, K. (1994). Determination of pore size and pore size distribution 1. Adsorbents and catalysts. *Journal of Membrane Science*, 96(4), 59–89. http://doi.org/10.1016/0376-7388(94)00126-x

Kercher, A. K., & Nagle, D.C. (2003). Microstructural evolution during charcoal carbonization by X-ray diffraction analysis. *Carbon*, 41, 15–27. http://doi.org/10.1016/S0008-6223(02)00261-0

Kumar, K.V., de Castro, M.M., Martinez-Escandell, M., Molina-Sabio, M., & Rodriguez-Reinoso, F. (2010). A Continuous Binding Site Affinity Distribution Function from the Freundlich Isotherm for the Supercritical Adsorption of Hydrogen on Activated Carbon. *The Journal of Physical Chemistry C*, *114*(32), 13759–13765. http://doi.org/10.1021/jp104014f

Kyzas, G. Z., Deliyanni, E. A., & Matis, K. A. (2016). Activated carbons produced by pyrolysis of waste potato peels: Cobalt ions removal by adsorption. *Colloids and Surfaces A: Physicochemical and Engineering Aspects,* 490, 74–83. https://doi.org/10.1016/j.colsurfa.2015.11.038

Langmuir, I. (1918). The Adsorption of Gases on Plane Surfaces of Glass, Mica and Platinum. *Journal of the American Chemical Society*, *40*(9), 1361–1403. http://doi.org/doi:10.1021/ja02242a004

Liao, B., Sun, W., Guo, N., Ding, S., & Su, S. (2016). Equilibriums and kinetics studies for adsorption of Ni (II) ion on chitosan and its triethylenetetramine derivative. *Colloids and Surfaces A: Physicochemical and Engineering Aspects*, 501, 32–41. http://doi.org/10.1016/j.colsurfa.2016.04.043

Lippens, B.C., Linsen, B.G., & de Boer, J. H. (1964). Studies on Pore Systems in Catalysts. The Adsorption of Nitrogen; Apparatus and Calculation. *Journal of Catalysis, 3*(1), 32–37. https://doi.org/10.1016/0021-9517(64)90089-2

Lippens, B.C., & de Boer, J. H. (1964)**.** Studies on Pore Systems in Catalysts III. Poresize distribution curves in aluminium oxide system. *Journal of Catalysis, 3*(1), 44-49. https://doi.org/10.1016/0021-9517(64)90091-0

Liu, Q. S., Zheng, T., Wang, P., Jiang, J. P., & Li, N. (2010). Adsorption isotherm, kinetic and mechanism studies of some substituted phenols on activated carbon fibers. *Chemical Engineering Journal, 157*(2-3), 348–356. http://doi.org/10.1016/j.cej.2009.11.013

Liu, T., Li, Y., Du, Q., Sun, J., Jiao, Y., Yang, G., ... & Zhu, H. (2012).Adsorption of methylene blue from aqueous solution by graphene. Colloids and Surfaces B: Biointerfaces, 90, 197–203. http://doi.org/10.1016/j.colsurfb.2011.10.019

Lowell, S., & Shields, J. E. (1991). *Powder Surface Area and Porosity.* (3rded.). NY: Chapman and Hall

Ma, L., Zhu, J., Xi, Y., Zhu, R., & He, H. (2016). Adsorption of phenol , phosphate and Cd (II) by inorganic – organic montmorillonites : A comparative study of single and multiple solute. *Colloids and Surfaces A: Physicochemical and Engineering Aspects*, 497, 63–71. http://doi.org/10.1016/j.colsurfa.2016.02.032

Mohd Din, A. T., Hameed, B. H., & Ahmad, A. L. (2009). Batch adsorption of phenol onto physiochemical-activated coconut shell. *Journal of Hazardous Materials, 161*(2-3), 1522–1529. http://doi.org/10.1016/j.jhazmat.2008.05.009

Molina-Sabio, M., Sánchez-Montero, M. J., Juarez-Galan, J. M., Salvador, F., Rodríguez-Reinoso, F., & Salvador, A.(2006). Development of porosity in a char during reaction with steam or supercritical water. *The journal of physical chemistry B*, 110 (25), 12360–4. http://doi.org/10.1021/jp0614289

Namasivayam, C., & Kadirvelu, K. (1997). Activated carbons prepared from coir pith by physical and chemical activation methods. *Bioresource Technology*, 62 (3), 123–127. http://doi.org/10.1016/S0960-8524(97)00074-6

Ngah, W. S. W., & Fatinathan, S. (2006). Chitosan flakes and chitosan- GLA beads for adsorption of p-nitrophenol in aqueous solution, *Journal of Colloids and Surfaces A: Physicochemical and Engineering Aspects*, 277, 214–222.

Pomonis, P. J., Petrakis, D.E., Ladavos, A. K., Kolonia, K.M., Pantazis, C.C., Giannakas, A. E., & Leontiou, A. A. (2005). The I-point method for estimating the surface area of solid catalysts and the variation of C-term of the BET equation. *Catalysis Communications, 6*(1), 93–96. http://doi.org/10.1016/j.catcom.2004.11.006

Pradhan, B. K., & Sandle, N. K. (1999). Effect of different oxidizing agent treatments on the surface properties of activated carbons. *Carbon,* 37(8),1323–1332. http://doi.org/10.1016/S0008-6223(98)00328-5

Rodriguez-Reinoso, F., Molina-Sabio, M., & Munecas, M. (1992). Effect of Microporosity and Oxygen Surface Groups of Activated Carbon in the Adsorption of Molecules of Different Polarity. *J. Phys. Chem*, 96, 2707–2713.

Shen, W., Li, Z., & Liu, Y. (2008). Surface Chemical Functional Groups Modification of Porous Carbon. *Recent Patents on Chemical Engineeringe,1*(1), 27–40. http://doi.org/10.2174/2211334710801010027

Simões, G., Hoffmann, C., Claudio, E., & Wilhelm, M. (2016). Preparation of novel adsorbents based on combinations of polysiloxanes and sewage sludge to remove pharmaceuticals from aqueous solutions. *Colloids and Surfaces A: Physicochemical and Engineering Aspects,* 497, 304–315. https://doi.org/10.1016/j.colsurfa.2016.03.021

Sing, K. (2001). The use of nitrogen adsorption for the characterisation of porous materials. *Colloids and Surfaces A: Physicochemical and Engineering Aspects*, 187–188, 3–9. https://doi.org/10.1016/S0927-7757(01)00612-4

Sreedhar, M.K., Madhukumar, A., & Anirudhan, T.S.(1999). Evaluation of an adsorbent prepared by treating coconut husk with polysulphide for the removal of mercury from wastewater. *Indian Journal of materiaial and Engineering Science*, 6, 279–285. http://nopr.niscair.res.in/handle/123456789/22330

Srivastava, V. C., Swamy, M. M., Mall, I. D., Prasad, B., & Mishra, I. M. (2006). Adsorptive removal of phenol by bagasse fly ash and activated carbon: Equilibrium, kinetics and thermodynamics. *Colloids and Surfaces A: Physicochemical and Engineering Aspects*, 272 (1-2), 89–104. https://doi.org/10.1016/j.colsurfa.2005.07.016

Stoeckli, F., López-Ramón, M.V., & Moreno-Castilla, C. (2001). Adsorption of phenolic compounds from aqueous solutions, by activated carbons, described by the dubinin - Astakhov equation. *Langmuir*, 17(11), 3301–3306. http://doi.org/10.1021/la0014407

Tan, I. A. W., Ahmad, A. L., & Hameed, B.H. (2008). Preparation of activated carbon from coconut husk: Optimization study on removal of 2,4,6-trichlorophenol using response surface methodology, *Journal of Hazardous Materials, 153*(1-2), 709–717. http://doi.org/10.1016/j.jhazmat.2007.09.014

Thomson, K.T., & Gubbins, K. E. (2000). Modeling Structural Morphology of Microporous Carbons by Reverse Monte Carlo. *Langmuir,* 16 (13), 5761–5773. http://doi.org/10.1021/la991581c

Vinod, V.P., & Anirudhan, T. S. (2002). Effect of experimental variables on phenol adsorption on activated carbon prepared from coconut husk by single-step steam pyrolysis: Mass transfer process and equilibrium studies. *Journal of Scientific & Industrial Research, 61*(2), 128–138. http://nopr.niscair.res.in/handle/123456789/17710

WHO. (1963). *International standards for drinking water.* Geneva: World Health Organization.

Zhao, J., Yang, L., Li, F., Yu, R., & Jin, C. (2009)**.** Structural evolution in the graphitization process of activated carbon by high-pressure sintering. *Carbon, 47*(3), 744–751. https://doi.org/10.1016/j.carbon.2008.11.006